Proceedings of the SEM Annual Conference
June 7-10, 2010 Indianapolis, Indiana USA

Effect of Aspect Ratio of Cylindrical Pulse shapers on Force Equilibrium in Hopkinson Pressure Bar Experiments

Sandeep Abotula[1] and Vijaya Chalivendra[2*]
[1]Dynamics Photo Mechanics Laboratory, University of Rhode Island, RI 02881
[2]Department of Mechanical Engineering, University of Massachusetts Dartmouth, MA 02747
[*]Corresponding author: vchalivendra@umassd.edu, 508-910-6572

ABSTRACT

A detailed experimental study was conducted in designing cylindrical pulse shapers for testing various types of materials using split Hopkinson pressure bar (SHPB) test setup. Copper-182 alloy and annealed C11000 was used as pulse shaper materials and six different types of pulse shapers for each case with their thickness to diameter (t/d) ratios ranging from 0.23 to 0.51 were used. Six types of materials namely Aluminum 6061-T6, Acrylic (Plexiglas), Ultra High Temperature Glass-Mica Ceramic (Macor), Ultra High Molecular Weight Polyethylene (UHMWPE), polyurethane and polyurethane syntactic foam were considered for testing. Inertial effects of pulse shapers play an important role in determining stress equilibrium in the specimen. The effect of t/d ratio of the pulse shaper on the force equilibrium condition at the specimen ends for above materials at a strainrate regime of 1000-2000/s was discussed and better pulse shapers for above materials were recommended.

INTRODUCTION

Pulse shaping has been used as a prominent technique for generating force equilibrium condition between incident and transmission bars in split Hopkinson pressure bar (SHPB) experimentation for the last one decade [1-3]. Force equilibrium is difficult to achieve when metallic SHPB setup is used to test both brittle and soft materials. The pulse shaping becomes very useful technique to ramp the incident pulse and generate force equilibrium conditions while testing above materials. Duffy *et al*. [4] were probably the first authors to propose the technique of pulse shaping. They used the pulse shaper in the form of a concentric tube to smooth pulses generated by explosive loading for the torsional Hopkinson bar. Franz *et al*. [5] and Follansbee [6] discussed various techniques for shaping the pulse and minimizing the dispersion of waves in the bars. Pulse shapers they used were slightly larger than the bars with 0.1-2.0 mm thick and the materials used for pulse shapers were paper, aluminum, brass or stainless steel. After these initial studies, the pulse shaping technique has been further investigated by several researchers recently. Nemat-Nasser *et al*. [7] recommended OFHC copper as pulse shaper to achieve ramp pulses for ceramics using SHPB. Chen *et al.* [8] used a polymer disk with elastomers to lengthen the incident compressive pulses. In addition to polymer disk as a pulse shaper, they also used a thin disk of annealed or hard C11000 copper to achieve ramp in the incident pulses for brittle materials that have failure strain less than 1.0%. Also Chen *et al*. [9] designed a combination of copper and mild-steel as a pulse shaper by experimental trials. The pulse shaper consists of two disks where steel end of the pulse shaper is attached to the incident bar and the striker impacts the copper end of the pulse shaper.

It can be noticed from above studies that copper has been successfully used as a pulse shaper in shaping incident pulse and generating force equilibrium conditions. It was identified from above studies that there was no detailed study conducted to understand the effect of pulse shaper aspect ratio (thickness/diameter) on the shaping of the incident pulse and initiation time of force equilibrium conditions. Hence this paper is mainly focused on studying the effect of the different aspect ratios of the pulse shapers on force equilibrium conditions when tests are conducted for different types of materials. Six types of materials namely Aluminum 6061-T6, Acrylic (Plexiglas), Ultra High Temperature Glass-Mica Ceramic (Macor), Ultra High Molecular Weight Polyethylene (UHMWPE), polyurethane and polyurethane syntactic foam are considered for testing. Both SHPB and modified SHPB with hollow transmission bar made out of Aluminum 7075-T651 are used in conducting this study.

T. Proulx (ed.), *Dynamic Behavior of Materials, Volume 1*, Conference Proceedings of the Society for Experimental Mechanics Series,
DOI 10.1007/978-1-4419-8228-5_69, © The Society for Experimental Mechanics, Inc. 2011

EXPERIMENTAL DETAILS

Table 1. Different types of pulse shapers

Pulse shaper type	Thickness (mm)	Diameter (mm)	Pulse shaper	t/d ratio
Type-1	No pulse shaper	--		--
Type-2	1.13	4.76	C182	0.237
Type-3	1.6	6.35	C182	0.251
Type-4	1.6	4.76	C182	0.336
Type-5	1.10	3.175	C 182	0.346
Type-6	3.00	6.35	C182	0.472
Type-7	1.6	3.175	C182	0.503
Type-8	1.13	4.76	C11000*	0.237
Type-9	1.6	6.35	C11000*	0.251
Type-10	1.6	4.76	C11000*	0.336
Type-11	1.10	3.175	C11000*	0.346
Type-12	3.00	6.35	C11000*	0.472
Type-13	1.6	3.175	C11000*	0.503

C11000*: Annealed C11000 alloy

Design of Pulse Shaper

Frew *et al*. [10] investigated analytically and specified a range of thickness to diameter (t/d) ratio of 0.16 to 0.5 for pulse shapers. Based on this specified range, in this study, six different types aspect ratios for both pulse shaper materials are designed as shown in Table-1. As given in Table-1, no pulse shaper is named as Type-1 and used as a reference. Type-2 to Type-13 has different t/d ratios by changing either thickness or diameter. The range of t/d ratios considered in this study is 0.237 to 0.503. High strength Copper (Alloy 182) and annealed C11000 was used as a material for pulse shapers.

Tested Materials

Six different materials namely Aluminum 6061-T6; Acrylic, also called Plexiglas; High-temperature Glass-filled Ceramic, also called Macor; Ultra-high molecular weight polyethylene (UHMWPE); Polyurethane; Polyurethane syntactic foam were considered for studying the effect of t/d ratio of the pulse shaper on the force equilibrium conditions. The above chosen materials fall in a wide spectrum of materials such as metal, brittle polymer, ceramic, ductile polymer, elastomer and foam. Identification of proper aspect ratio of pulse shapers for these materials in this study will help the researchers to choose appropriate type of pulse shaper while conducting experiments of similar type of materials. Polyurethane (supplied by Hapflex Inc., MA, USA) is thermoset polymer, which consists of two parts, part-A: resin and part-B: Hardener. Polyurethane syntactic foam is made using same above polyurethane with 30% weight fraction of gas bubbles (supplied by 3M, MA, USA). The pulse shaper for one type of material would not be same for all other types of materials due to fact that above materials do not have same impedance.

Experimental Procedure

In order to perform low-strain rate testing on all proposed materials, both traditional and modified SHPB setups are employed. Traditional SHPB consists of a striker, an incident bar and a transmission bar and they are all made of aluminum 7075-T651 as shown in Figure 1. The striker bar used in these experiments has a diameter of 12.7mm and length 203.2mm. Incident and transmission bars have the diameter of 12.7 mm and length up to 1220mm. A pulse shaper of different dimensions listed in the above section is placed using KY jelly at the impact end of the incident bar as shown in Figure 1. The specimen is sandwiched between incident bar and transmission

bar. Specimen has the thickness of 3mm and diameter of 6.35mm. Molybdenum disulfide lubricant is applied between specimen and the contacting surfaces of bars to minimize the friction.

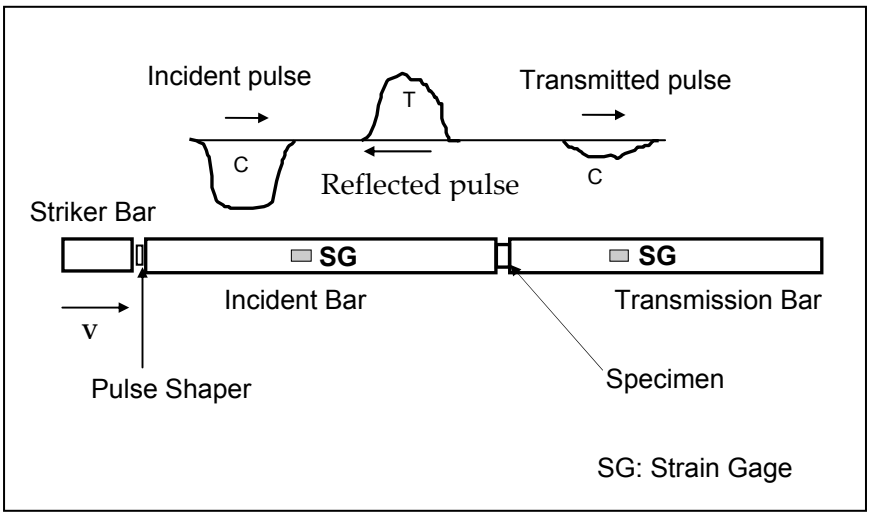

Figure 1. Experimental setup of SPHB

For characterizing low-impedance materials such as Plexiglas, Macor, UHMWPE, Polyurethane and Polyurethane foam, a modified SHPB is used. This setup has hollow transmission bar, which provides a decent compressive pulse while testing the above mentioned low impedance materials. An aluminum end cap is press fitted into the hollow tube to support the specimen at the specimen transmission bar interface. Same Aluminum 7075-T651 alloy was used for hollow transmission bar. The transmission bar has the outside diameter of 12.7mm and inside diameter of 9.5mm with incident bar (A_i) to transmission bar (A_t) area ratio of $\frac{A_i}{A_t} = 2.28$ [8].

When striker bar impacts the incident bar, an elastic compressive stress pulse, referred as incident pulse is generated. The generated pulse deforms the pulse shaper at the impact end and creates a ramp in the incident pulse which further propagates along the incident bar. When the incident pulse reaches the specimen, some part of it reflects back into the incident bar (reflected pulse) in the form of tensile pulse due to the impedance mismatch at the bar-specimen interface and the remaining part is transmitted (transmission pulse) to the transmission bar. Axial strain gauges mounted on the surfaces of the incident and transmission bar provide time-resolved measures of the elastic strain pulses in the bars.

Experiments were carried out at an strainrate regime of 1000-2000/s for all six different types of materials. Different striker lengths and pressures were used for different materials to obtain the above said strainrate.

Force equilibrium within the specimen during the wave loading is attained when forces on each face of the specimen are equal. From Nicholas [2] and Gray [11], the expressions for the forces at the specimen incident bar interface and at the specimen transmission bar interface are given equations (1) and (2) respectively.

$$F_i = A_b E_b (\varepsilon_i + \varepsilon_r) \quad (1)$$

$$F_t = A_b E_b \, \varepsilon_t \quad (2)$$

Where A_b is cross-sectional area of incident bar; E_b is Young's modulus of the bar material; ε_i, ε_r, ε_t are time-resolved strain values of the incident, reflected and transmitted pulses respectively.
When these two forces in equations (1) & (2) are equal, then the specimen is said to be in dynamic force equilibrium. The ratio of these two forces as given in equation (3) provides a measure for force equilibrium. For ideal equilibrium conditions, the ratio should be 1.0.

$$F_i / F_t = (\varepsilon_i + \varepsilon_r) / \varepsilon_t \quad (3)$$

In the following experimental results section, the effect of aspect ratio of pulse shaper is discussed by plotting the force ratio given in equation (3) as function of specimen loading time. The initiation time for force equilibrium upon loading the specimen and the extent of force equilibrium during whole loading duration is discussed.

EXPERIMENTAL RESULTS

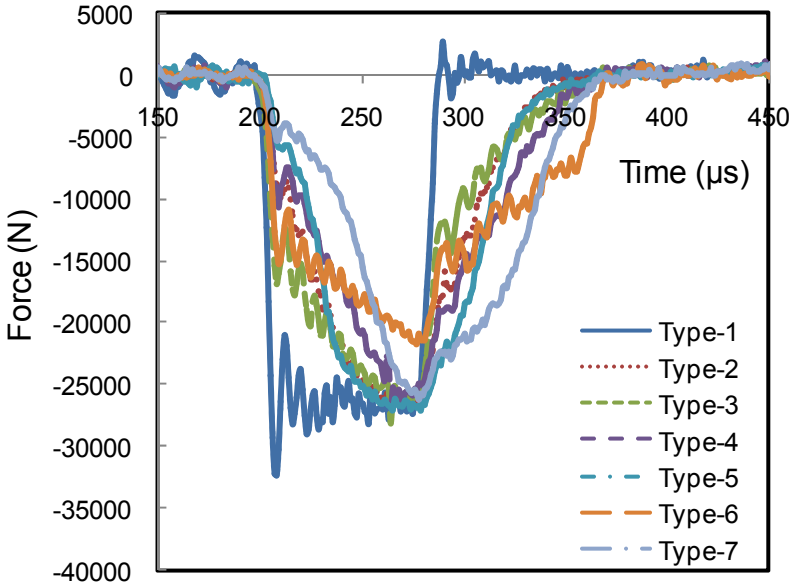

Figure 2. Typical incident pulses for different types of pulse shapers

As discussed in the above section, the pulse shaper should generate a ramped incident compressive pulse for gradual loading of the test specimen which is sandwiched between two bars. Figure 2 shows the typical incident pulses obtained from the experiments for different aspect ratios of C182 alloy pulse shaper. It can be noticed that for Type-1 which is the case for no pulse shaper, the incident pulse has no ramp and the maximum force is attained in less than 10μs, so the specimen does not have much time to reach equilibrium. For all other types of pulse shapers, it takes approximately 50μs to reach the maximum force, and thus allowing sufficient time for the specimen to be in equilibrium. It can be noticed that the length of the pulse increases with pulse shapers against the no pulse shaper (Type-1). Similar case was observed for annealed C11000 alloy pulse shaper. From Figure 2, it can be seen that, as the diameter of the pulse shaper increases, it provides very good ramp in the incident pulse. Also as the thickness of the pulse shaper increases, the rising time of the incident pulse increases. So from the designed pulse shapers, Type-5 (thickness=1.10mm, diameter = 3.175mm and t/d = 0.346) pulse shaper provided very good ramp and long rising time in the incident pulse. However, the pulse shaper with this aspect ratio may not provide good equilibrium for all the materials since the time required in reaching equilibrium is different for different materials and also it depends on the impedance mismatch between the specimen-bar interfaces. The ratio of mechanical impedance of the specimen to bars (β) is given by,

$$\beta = \frac{A\rho c}{A_0 \rho_0 c_0} \quad (4)$$

Where A, ρ and c are the area, density and wave speed of the specimen respectively and A_0, ρ_0 and c_0 represents area, density and wave speed of the pressure bars. ρc defines mechanical impedance. As the impedance mismatch between the specimen-bar interfaces increases, the value of β decreases. The number of reverberations (n) required for the specimen to attain equilibrium is given by,

$$n = \frac{c * t}{L} \tag{5}$$

Where *t* represents the time required for the specimen to reach equilibrium in μs and *L* represents the length of the specimen [12]. To attain equilibrium, the loading pulse has to travel *n* times from one end to other end of the specimen.

Table 2. Ratio of impedances of different material to pressure bars

Material	β
Al 6061-T6	$\approx \frac{1}{4}$
Plexiglas	$\approx \frac{1}{30}$
Macor	$\approx \frac{1}{6} - \frac{1}{4}$
UHMWPE	$\approx \frac{1}{100}$
Polyurethane Elastomer	$\approx \frac{1}{1000}$
Polyurethane Foam	$< \frac{1}{1000}$

Table 2. shows the ratio of mechanical impedance of specimen to bar for different materials tested in this paper. From the table, it can be observed that the value of β decreases for soft materials. So it can be assumed that attaining equilibrium will be difficult for the softer (low impedance) materials.

The dimensions of the pulse shapers are also restricted. The diameter of the pulse shaper after impact cannot exceed than the bar diameter. Also if the thickness of the pulse shaper is too large, it absorbs maximum amount of energy from the striker and transmits very less energy to the incident bar. The rise time of the pulse also increases with thicker pulse shapers and this may lead to the overlapping of the pulses when tested at low strain rates. So it is not advisable to use thicker pulse shapers.

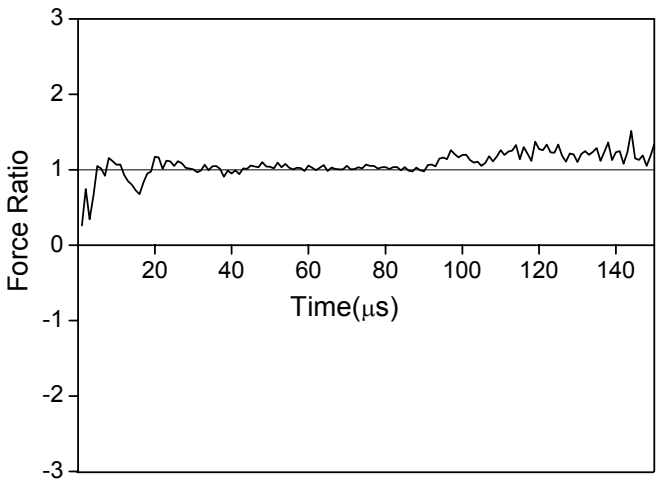

Figure 3. Force equilibrium condition of Al 6061-T6 using Type 2 pulse shaper

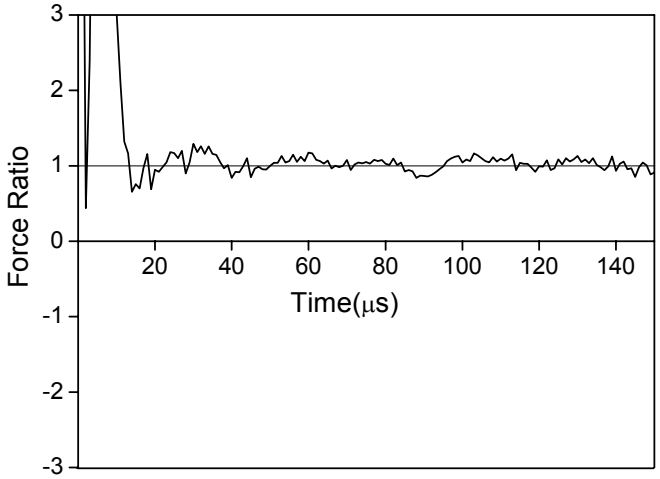

Figure 4. Force equilibrium condition of Plexiglas using Type 5 pulse shaper

For all the materials tested in this study, due to brevity of space only pulse shapers that generated the best force equilibrium condition were reported in this paper. The solid line in all the figures represents the ideal force ratio of 1.0. All the pulse shapers tested provided better equilibrium than the case of no pulse shaper but only certain aspect ratio of pulse shaper provided equilibrium for the entire loading duration. Figure 3 shows the force ratio of Al 6061-T6 using Type-2 (thickness=1.13mm, diameter=4.76mm and t/d=0.237) pulse shaper. It can be noticed from the figure that the selected pulse shaper provides the force ratio that is very close to 1.0 for most of the specimen loading time and their force equilibrium initiates at around 5μs. As Aluminum 6061-T6 is tested with Al 7075-T4 bars, the impedance mismatch between the specimen and pressure bars is very less and it helped in attaining very good equilibrium even at early stage of loading.

Figure 4 shows the force ratio for acrylic (Plexiglas) material using Type-5 (thickness=1.10mm, diameter=3.175mm and t/d=0.346) pulse shaper. Type-5 pulse shaper attains the force equilibrium at around 17μs upon starting of the loading of the specimen. Due to the significant difference in the impedance mismatch of Plexiglas (refer Table 2) with respect to pressure bars, it became difficult to get equilibrium at early stages. After the equilibrium is achieved, It maintains for rest of the loading duration.

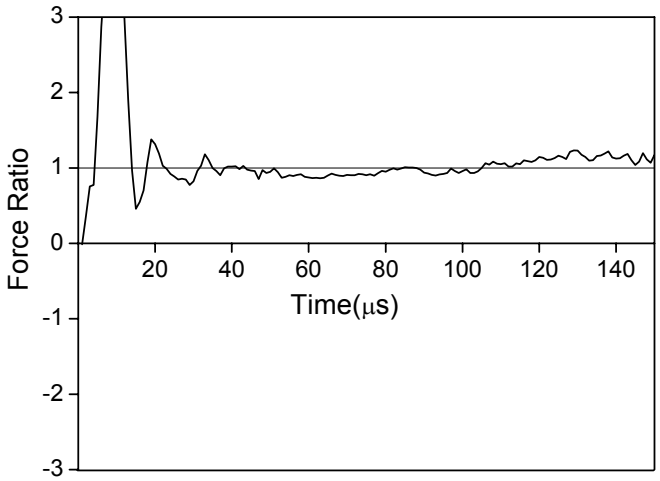

Figure 5. Force equilibrium condition of Macor using Type 5 pulse shaper

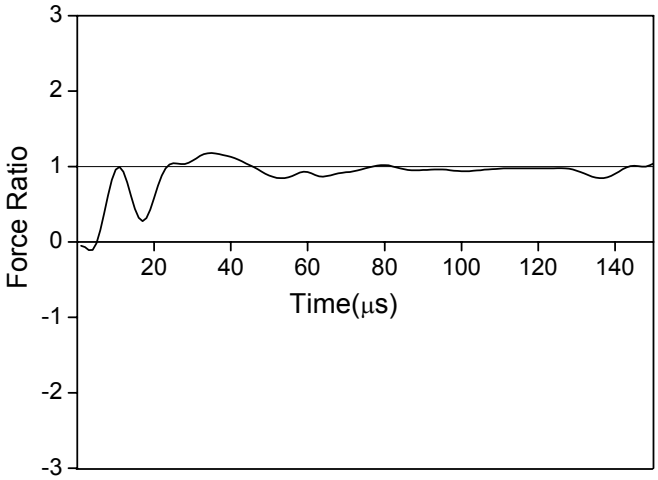

Figure 6. Force equilibrium condition of UHMWPE using Type 11 pulse shaper

Force ratio curves for ultra-high temperature glass-mica ceramic (Macor) for the pulse shaper Type-5 is shown in Figure 5. Macor is a brittle ceramic and having force equilibrium condition before the specimen breaks under dynamic loading conditions is essential for meaningful dynamic compressive strength value. Type-5 pulse shaper attains the force equilibrium at around 14μs. As in the case of Plexiglas, due to significant difference in the impedance mismatch, no equilibrium was achieved before 14μs. Macor reached equilibrium little early than Plexiglass since impedance mismatch of Macor with respect to output bars is less when compared to Plexiglas. It also maintains the equilibrium for the rest of the loading duration.

Figure 6 shows the force ratio curve for ultra high molecular weight polyurethane (UHMWPE) specimen using Type-11 (thickness = 1.10mm, diameter = 3.175mm and t/d = 0.346) pulse shaper. UHMWPE is a semi-crystalline, ductile polymer. It has high impedance mismatch with respect to Aluminum 7075-T651. So it took much time to reach equilibrium (at around 24μs) than the other materials and maintained decent equilibrium till the rest of the loading duration.

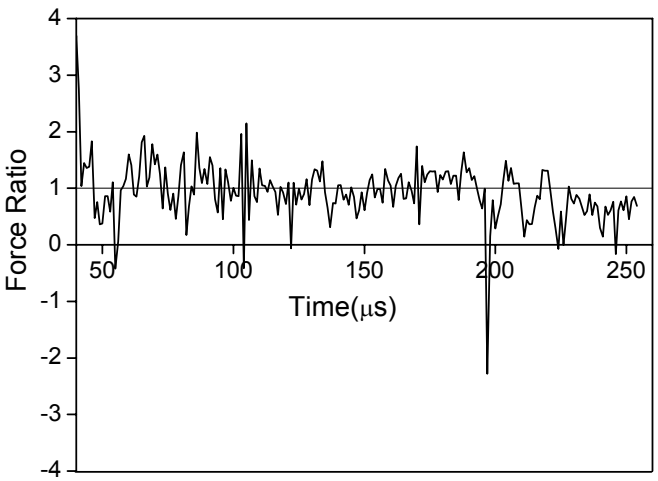

Figure 7. Force equilibrium condition of Polyurethane using Type 10 pulse shaper

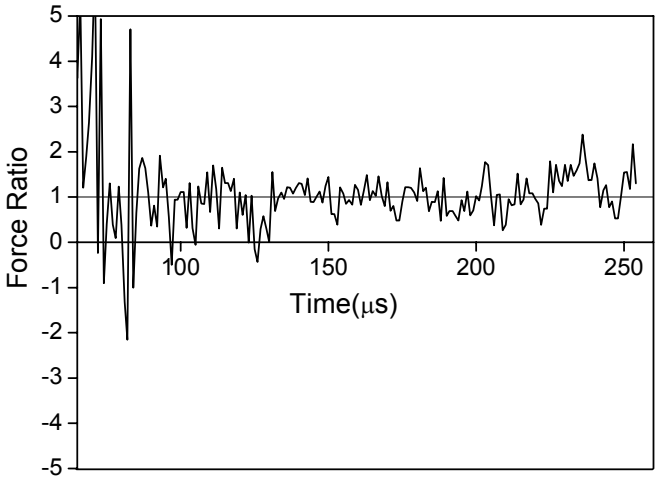

Figure 8. Force equilibrium condition of Polyurethane syntactic foam using Type 9 pulse shaper

Force ratio curve for polyurethane elastomer using Type-10 (thickness = 1.6mm, diameter = 4.76mm and t/d = 0.336) pulse shaper is shown in Figure 7. Since the impedance of polyurethane is very low when compared to Aluminum 7075-T651, it is expected that attaining force equilibrium condition is very difficult. Due to the low mechanical impedance, nearly all the compressive wave is reflected back in the form of tensile to the incident bar and very less is transmitted to the transmission bar. The oscillations in the figure are due to very low magnitude of transmission pulse. It can be seen from the figure that, equilibrium was achieved only after 50μs indicating that experimental result was valid only after this time [13]. This proves that attaining equilibrium at early stages of loading is very difficult for soft materials. So due to several oscillations of force ratio curve shown in Figure 7, exact initiation time of force equilibrium condition for polyurethane specimens is not reported.

Figure 8 shows the force ratio curve for polyurethane syntactic foam specimens using Type-9 (thickness = 1.6mm, diameter = 6.35mm and t/d = 0.251) pulse shaper. Even for this material as in the case of polyurethane elastomer, equilibrium was not achieved until 70μs [13]. As this material is much softer and has very high mechanical impedance, it took more time than polyurethane elastomer to reach equilibrium. Due to several oscillations of force ratio curve for Type-9 pulse shaper as shown in Figure 9, again the exact initiation of force equilibrium condition for polyurethane syntactic foam specimen is not reported. Better equilibrium can be achieved by reducing the thickness of the specimen but they were some limitations on thickness restrictions of the specimen.

Table 3. Number of reverberations of different material to reach equilibrium

Material	***Number of reverberations***
Al 6061-T6	8
Plexiglas	9
Macor	21
UHMWPE	5
Polyurethane Elastomer	3
Polyurethane Foam	3

Table 3. shows the number of reverberations for different materials to reach equilibrium. For AL 6061-T6, due to less impedance mismatch, it took 8 reverberations to reach equilibrium. From the table, it can be noticed that Macor takes 21 reverberations (higher than other materials) even though it took less time to reach equilibrium than other materials because the wave speed of Macor is much greater than the other materials. Since the value of n increases with the wave speed and L being constant for all materials, materials with higher wave speed will have higher value of n. So it can be concluded here that due to high wave speed, some materials may have larger value of n but still it takes less time to reach equilibrium. On the contrast, if the wave speed of the material is less, then it takes much time for less number of reverberations.

CONCLUSIONS

In this paper, a detailed experimental study was conducted to investigate the effect of thickness to diameter ratio of the copper-182 alloy and annealed C11000 pulse shaper on force equilibrium conditions for six different types of materials. Following are the major outcomes of this study:

- For Aluminum 6061-T6, Type-2 pulse shaper provided force equilibrium initiation time at around 5μs and maintained equilibrium conditions for entire loading duration.
- For acrylic (Plexiglass) specimens, Type-5 initiated the equilibrium conditions at around 17μs and conditions were maintained for entire loading duration.
- For Macor specimens, Type-5 pulse shaper attains the force equilibrium at around 14μs and also maintains the equilibrium for the rest of the loading duration.
- For UHMWPE, Type-11 pulse shaper provided force equilibrium conditions. The initiation time of the equilibrium is at around 24μs and maintained till 150μs.
- For Polyurethane and syntactic foam materials, Type-10 and Type-9 respectively provided decent equilibrium conditions with several oscillations around desired force ratio of 1.0. The equilibrium was only achieved after 60μs proving that it is very difficult to get equilibrium for soft materials at early stages of loading.

REFERENCES

[1] Kolsky, H. An Investigation of the Mechanical Properties of Materials at very High Strain Rates of Loading. *Proceeding of Physics Society,* **62**, 676-700, 1949.

[2] Nicholas, T.: Material Behavior at High Strain Rates. *Impact Dynamics, Chap. 8, John Wiley & Sons, New York,* 1982.

[3] Davies, E. D. H. and Hunter, S. C.: The Dynamic Compression Testing of Solids by the method of the Split Hopkinson Pressure Bar. *Journal of the Mechanics and Physics of Solids,* **11**, 155-179, 1963.

[4] Duffy, J., Campbell, J. D., and Hawley, R. H.: On the Use of a Torsional Split Hopkinson Bar to Study Rate Effects in 1100-0 Aluminum. *ASME Journal of Applied Mechanics,* **37**, 83-91, 1971.

[5] Franz, C. E., Follansbee, P. S., and Wright, W. J.: New Experimental Techniques with the Split Hopkinson Pressure Bar. *8th international conference*, *ASME,* 1984.

[6] Follansbee, P. S.: The Hopkinson Bar Mechanical Testing, *metals handbook, 9th ed., ASM*, Metals Park, Ohio. **8**, 198-217, 1985.

[7] Nemat-Nasser, S., Issacs, J. B., and Starret, J. E.: Hopkinson Techniques for Dynamic Recovery Experiments. *Proceeding of Royal society of London, A*. **435**, 371-391, 1991.

[8] Chen, W., Zhang, B. and Forrestal, M. J.: A Split Hopkinson Bar Technique for Low-Impedance Materials. *Experimental Mechanics,* **39**, 81-85, 1999.

[9] Chen, W., Song, B., Frew, D. J., and Forrestal, M. J.: Dynamic Small Strain Measurements of a metal Specimen with a Split Hopkinson Pressure Bar. *Experimental Mechanics,* **43**, 20-23, 2003.

[10] Frew, D. J., Forrestal, M. J., and Chen, W.: Pulse Shaping Techniques for Testing Brittle Materials with a Split Hopkinson Pressure Bar. *Experimental Mechanics,* **42**, 93-106, 2002.

[11] Gray, G. T.: Classical Split-Hopkinson Pressure Bar Technique. ASM handbook, **8**, Mechanical Testing and Evaluation, *ASM International*, Materials Park, OH, 44073-0002, 2000.

[12] Yang, L.M., Shim, V. P. W.: An Analysis of Stress Uniformity in Split Hopkinson Pressure Bar Test Specimens. *International Journal of Impact Engineering*, **31**, 129-150, 2005.

[13] Song, B., Chen, W and Jiang, X., Split Hopkinson Pressure Bar Experiments on Polymeric Foams. *International of Journal Vehicle Design*, **37**, 185-198, 2005.